Leukemia Research 87 (2019) 106264

Contents lists available at ScienceDirect

Leukemia Research

journal homepage: www.elsevier.com/locate/leukres

Letter to the Editor

Functional evaluation of isocitrate dehydrogenase 1 and 2 variants of unclear significance in chronic myeloid neoplasms

Substantial advances have been made regarding the range and depth of clinical gene sequencing platforms, resulting in easier detection of known cancer-specific mutations. Additional genetic variants are also being identified in genes known to be pathogenic in cancer, but not functionally characterized and not represented in normal populations. Predicting the potential pathogenicity of these variants with 'unclear clinical significance' (VUS) on protein structure and function is difficult, and increases the challenge of employing molecular markers to effectively define risk assessment and assign specific therapy regimens.

We have identified several VUS predicted as pathogenic and/or damaging in isocitrate dehydrogenase 1 and 2 (*IDH1/IDH2*) using available *in-silico* algorithms (SIFT/MutationTaster) in patients with chronic myeloid malignancies. Key mutations in these genes result in the known production and accumulation of an aberrant oncometabolite (2-hydroxyglutarate), which disrupts the epigenetic phenotype of myeloid cells and results in progression and transformation of disease [1]. Mutant IDH inhibitors have shown clinical utility both as single agents and in combination strategies for affected patients, and therefore, assessing the functional effect of *IDH1/2* VUS is important [2,3]. For this study, we used highly sensitive mass spectrometry approaches to measure and compare levels of IDH metabolites in *IDH* VUS to those with known *IDH* mutations. We also analyzed the potential protein structural consequences of *IDH* variants using protein-based secondary structure prediction and 3D-modeling of IDH-specific crystal structure.

IDH1 and *IDH2* each encode an isoform of a key metabolic enzyme that participates in a carefully regulated irreversible step in the citric acid cycle (TCA), producing alpha-ketoglutarate (α-KG). Normal function of this pathway is essential for the generation of accessible cellular energy in the form of NAPDH, as well as participation in biosynthesis of glucose, fatty acids, and amino acids. Mutations affecting *IDH1* and *IDH2* prevent the forward conversion of $NADP^+$ to NADPH (a loss-of-function effect), and this encourages the reverse reaction, resulting in an acquired (gain-of-function) ability to reduce α-KG to 2-hydroxyglutarate (2-HG) -specifically, the D-2-HG isomer structure. The latter is an oncogenic competitive inhibitor of α-KG-dependent enzymes, including histone demethylases and the TET family of 5-methylcytosine hydroxylases, and leads to altered DNA methylation [1,4]. Current known *IDH* mutations are mapped to the active site of the enzyme and include three specific arginine residues: R132 (*IDH1*), and R140, R172 (*IDH2*) [5]. Mutations affecting these residues have been described in myeloid malignancies, including in up to 20% of acute myeloid leukemia (AML), in up to 5% of myelodysplastic syndromes (MDS) and myeloproliferative neoplasms (MPN), and around 9% in overlap syndromes (MDS/MPN) [5–12]. Mutations at *IDH2* residue R172 are the least frequent [9,13,14].

Methods: After institutional approval, bone marrow DNA from patients with MDS, MPN, and MDS/MPN overlap syndromes were subjected to next generation sequencing (29-gene panel, including the entire coding region of *IDH1/2*) by previously described methods [15]. From this cohort, we analyzed a sub-set of patients with available EDTA-preserved plasma [wild-type *IDH* (n = 20), *IDH* mutant (n = 43) and *IDH* VUS (n = 9; with ≤0.03% normal frequency and predicted damaging *in-silico* scores by either/or SIFT and MutationTaster)] and normal controls (n = 3) for LC/MS based detection of IDH-related metabolites; D and L isomers of 2-HG, α-KG, and total 2-HG [See Fig. 1]. The crystal structure and location of each variant was provided by the RCSB Protein Data Bank. Values for amino acid side chain volumes were taken from Zamyatnin [16]. The impact of variants on protein secondary structure elements (beta strand, alpha helix, and random coil) was assessed using the GorIV secondary structure prediction algorithm, and an assessment of the effects within the context of the tertiary structure was performed in PyMOL [See Supplemental Table 3 for details on all programs].

For IDH-metabolite detection, the concentration of α-KG and 2-HG were measured by gas chromatography-mass spectrometry, (GC/MS) as previously described [Supplemental Methods] [17,18]. Concentrations of L and D isomers of 2-HG were separated and quantified by liquid chromatography coupled with mass spectrometry (LC/MS) as previously described [Supplemental Methods] [19,20]. The standard t-test was used to calculate significance between case groups. All statistical analyses considering clinical parameters was completed using either the Mann–Whitney or Kruskal–Wallis test, and calculation of overall survival (OS) -from the date of first referral to the date of death (uncensored) or last contact (censored)- was performed using Kaplan–Meier method with log-rank comparison by Chi-Square.

Results: One hundred and nine cases containing either an *IDH* mutation or VUS were included in the study, with the median age being 68 years (range, 39–94) and 69% male. Of these, 35% had MDS (n = 38), 36% had MPN (n = 39), and 29% had MDS/MPN overlap syndromes (n = 32). Eighty percent (n = 87) had a pathogenic *IDH* mutation, including 26% with *IDH1*R132[C/G/H/S] (n = 28; 11 MDS, 8 MPN, 9 MDS/MPN) and 54% with *IDH2*R140[G/Q/W/*] (n = 59; 23 MDS, 20 MPN, 16 MDS/MPN). *IDH* VUS were detected in 20% [n = 22] cases, involving *IDH1* in 5% [n = 5] cases and *IDH2* in 15% [n = 17] cases. In total, there were fourteen unique VUS [see Fig. 1A, Supplemental Fig. 1]. One patient with MPN had dual presence of an *IDH1* mutation and *IDH2* VUS (T435M) and was considered mutant for this study. Four *IDH* mutant and two VUS cases (*IDH1*R119W and *IDH2*A416S) also had mutations in *TET2*. All *IDH* VUS were missense except for one case with a 2 amino acid insertion in *IDH2* (R149_E150insSR). The most frequent VUS observed was *IDH2*T352P (n = 8; 7%). Seventeen of twenty additional *IDH* wild-type cases used in LC–MS testing (10 MDS and 10 PMF each) were included for OS comparison (9 MDS and 8 PMF).

LC–MS analysis was performed on 72 cases with available plasma (*IDH* mutant [n = 43], *IDH* VUS [n = 9], *IDH* wild-type [n = 20], and n = 3 normal plasma were used for control). We found no statistical

https://doi.org/10.1016/j.leukres.2019.106264
Received 10 October 2019
Available online 24 October 2019

A.

Gene	Residue Change	Type	VAF (%)	LC-MS (n)	Total Clinical Annotated (n)	Nucleotide change	dbSNP	SIFT	MutationTaster	ExAC
IDH1	**C379Y**	VUS	52%		1	*c.1136G>A*	no	Deleterious (score: 0.2)	Disease Causing (p-value: 1)	no
IDH1	**E110K**	VUS	47%	1	1	*c.328G>A*	rs775517144	Deleterious (score: 0)	Disease Causing (p-value: 1)	no
IDH1	**I189V**	VUS	52%	1	1	*c.565A>G*	rs62193615	Deleterious (score: 0)	Disease Causing (p-value: 1)	0.03%
IDH1	**R119W**	VUS	46%	1	1	*c.355C>T*	rs747419787	Deleterious (score: 0)	Disease Causing (p-value: 1)	<0.01%
IDH1	**V121M**	VUS	8%	1	1	*c.361G>A*	no	Deleterious (score: 0)	Disease Causing (p-value: 1)	no
IDH2	**V335I**	VUS	49%		1	*c.1003G>A*	rs140596855	Tolerated (score: 0.09)	Disease Causing (p-value: 0.998	0.03%
IDH2	**T352P**	VUS	45%*	3	8	*c.1054A>C*	rs770548230	Deleterious (score: 0)	Disease Causing (p-value: 1)	no
IDH2	**A416S**	VUS	11%	1	1	*c.1246G>T*	rs776562578	Tolerated (score: 0.31)	Disease Causing (p-value: 1)	no
IDH2	**T117N**	VUS	17%		1	*c.350C>A*	no	Deleterious (score: 0.04)	Disease Causing (p-value: 1)	no
IDH2	**R149_E150insSR**	VUS	5%		1	*c.446_447insATCTCG*	no			no
IDH2	**H175L**	VUS	53%		1	*c.524A>T*	rs1261644524	Tolerated (score: 0.27)	Disease Causing (p-value: 0.99)	no
IDH2	**V217M**	VUS	53%	1	1	*c.649G>A*	rs745751309	Deleterious (score: 0.03)	Disease causing (p-value: 0.987)	<0.01%
IDH2	**D225N**	VUS	44%**		2	*c.673G>A*	rs142816010	Deleterious (score: 0)	Disease Causing (p-value: 1)	0.02%
IDH2	**E226K**	VUS	57%		1	*c.676G>A*	rs576407061	Deleterious (score: 0)	Disease Causing (p-value: 1)	<0.01%
IDH1	**R132C**	MUT		7	8	*c.394C>T*	rs121913499	Deleterious (score: 0)	Disease Causing (p-value: 1)	no
IDH1	**R132G**	MUT			2	*c.394C>G*	rs121913499	Deleterious (score: 0)	Disease Causing (p-value: 1)	no
IDH1	**R132H**	MUT		7	13	*c.395G>A*	rs121913500	Deleterious (score: 0)	Disease Causing (p-value: 1)	<0.01%
IDH1	**R132S**	MUT		4	5	*c.394C>A*	rs121913499	Deleterious (score: 0)	Disease Causing (p-value: 1)	no
IDH2	**R140G**	MUT		1	1	*c.418C>G*	rs267606870	Deleterious (score: 0.01)	Disease Causing (p-value: 1)	no
IDH2	**R140***	MUT		1	1	*c.418_419; CG>TA*	rs267606870	Deleterious (score: 0)	Disease Causing (p-value: 1)	no
IDH2	**R140W**	MUT		2	5	*c.418C>T*	rs267606870	Deleterious (score: 0)	Disease Causing (p-value: 1)	no
IDH2	**R140Q**	MUT		21	51	*c.419G>A*	rs121913502	Deleterious (score: 0.03)	Disease Causing (p-value: 1),	<0.01%
IDH2	**R172K**	MUT			1	*c.515G>A*	rs121913503	Tolerated (score: 0.11)	Disease Causing (p-value: 1)	no

* T352P VAF of additional *n*=7: (40%,36%,33%,42%,31%,46%,35%)

**D225N VAF of additional n=1: (51%)

B.

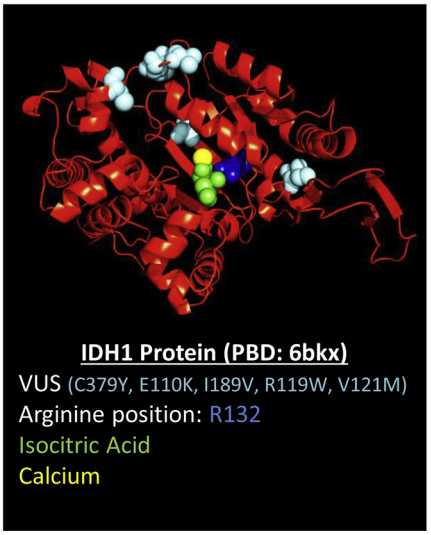

C.

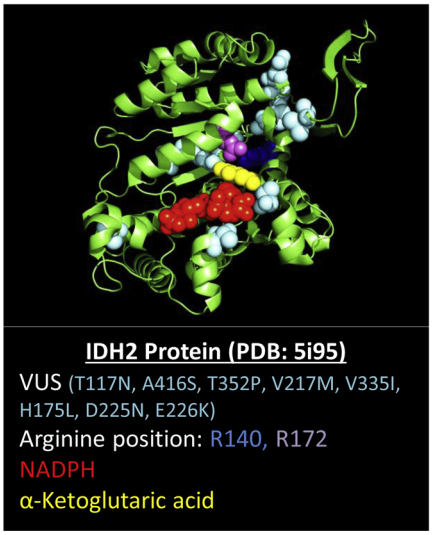

Fig. 1. Details and Location of Individual IDH Mutant/VUS. The details for IDH1 & 2 mutations and VUS included in study are listed in panel (A) and include: nucleotide and amino acid residue change, variant allele frequency (VAF), number of cases tested by LC–MS, in silico protein prediction (both SIFT and MutationTaster), population frequency (ExAC), and dbSNP ID. Panels (B&C) include RCSB Protein Bank generated image of IDH1 (B) and IDH2 (C) 3D crystal structure highlighting the proximity of VUS (light blue) to essential biological compounds for IDH activity (yellow, green, red –see key under each panel) and pathogenic mutations (dark blue and purple) (For interpretation of the references to colour in this figure legend, the reader is referred to the web version of this article).

difference in the levels of α-KG, the metabolite produced during normal homeostasis, between any of the groups: *IDH* mutant (avg: 8.6 μM, SD: 4.53), *IDH* VUS (avg: 9.3 μM, SD: 4.34), *IDH* wild-type (avg: 7.0 μM, SD: 3.94), and control (avg: 5.40 μM, SD: 0.36) [Fig. 2C and Supplemental Table 1]. However, we detected levels of the oncometabolite 2-HG in all *IDH* mutant cases (avg: 24.4 μM, SD: 31.7, range: 0.58–182.8 μM) which was significant over both *IDH* VUS (avg: 1.2 μM, SD: 0.49, $p = 0.034$*) and *IDH* wild-type (avg: 1.4 μM, SD: 1.1, $p = 0.0020$**) cases [Fig. 2D and Supplemental Table 1]. There was no significant difference in levels between *IDH1* vs *IDH2* VUS types. The levels of D-2-HG, the enantiomer associated with aberrant 2-HG production, was significantly increased in *IDH* mutant cases (avg: 21.9 μM, SD: 32.92, range: 0.53–199 μM) over wild-type (avg: 0.6 μM, SD: 0.25, $p = 0.0055$**), however, did not quite reach statistical significance with *IDH* VUS cases (avg: 0.6 μM, SD: 0.17, $p = 0.06$), most likely due to low number, since the largest value for an *IDH* VUS was still less than 1μM. There was no change seen in L-2-HG [Fig. 2E & F and Supplemental Table 1].

On a univariate analysis, there was a trend towards an inferior OS in cases with mutant *IDH* (35 months), in comparison to *IDH* VUS cases (50 months, $p = 0.0553$) and those that were *IDH* wild-type (66 months, $p = 0.0543$), with no differences in OS between *IDH* VUS and *IDH* wild-type cases [Fig. 2A]. Considering *IDH1* VUS and *IDH2* VUS separately, cases with *IDH2* VUS (77 months) had superior OS compared to mutant *IDH* (34.8 months, $p = 0.0312$*), while *IDH1* VUS cases had an OS similar to mutant (36.5 months) [See Fig. 2B]. In comparison to mutant *IDH*, cases with *IDH* VUS were associated with a lower frequency of *SRSF2* mutations (57.4% vs 23.5%, $p = 0.0117$*), however, no other significantly different clinical values were observed (see Supplemental Table 2).

The mutant-targeted arginine residues (R132, R140, and R172) are in close proximity to the protein-catalytic center and key interaction partners: isocitric acid, calcium, and α-KG. Almost all of the *IDH* VUS in this study were located away from the active center and were therefore allosteric in nature [Fig. 1B & C, and Supplemental Fig. 1 and Table 4]. Most of these VUS potentially affect secondary and/or tertiary structure of the protein probably resulting in a destabilization or (partial) misfolding of the protein, thereby potentially impacting function (functional studies to validate these observations are needed -see Supplemental Table 4).

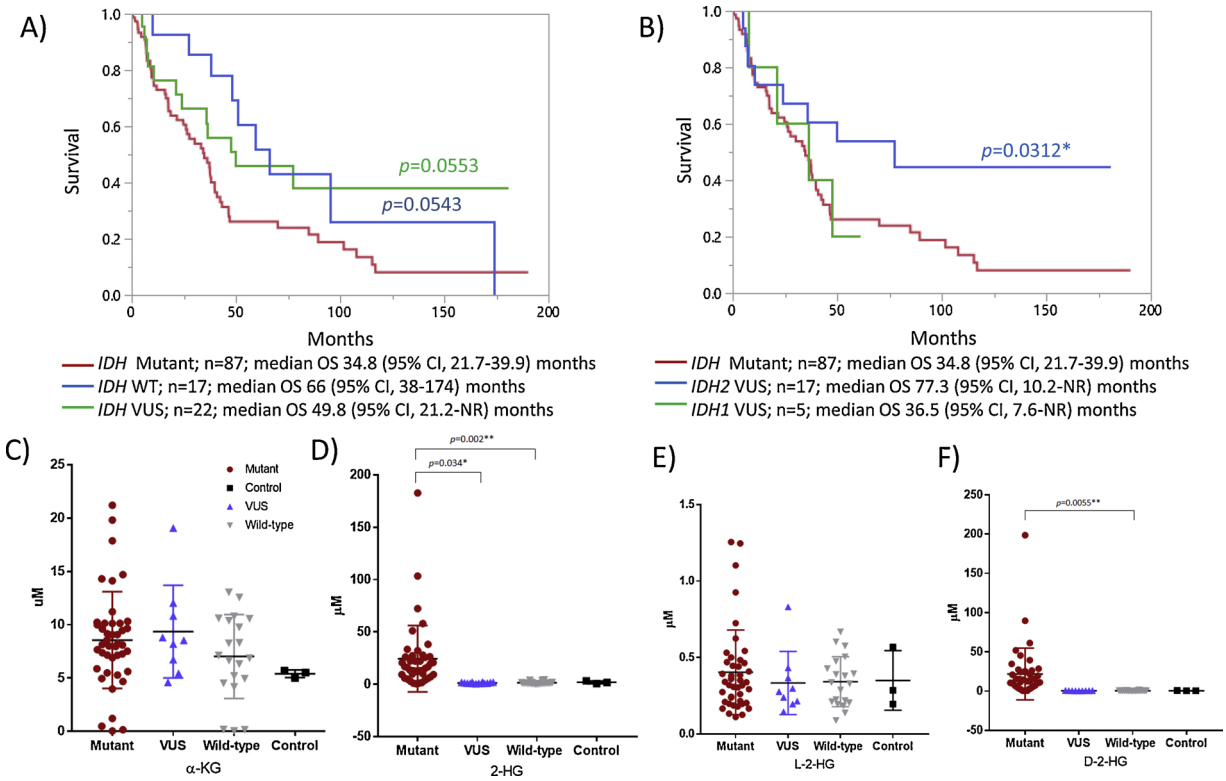

Fig. 2. Overall Survival and Metabolite Quantification of IDH Mutant/VUS. Panels (A–B) include Kaplan Meier OS curve for *IDH* mutant vs. VUS and IDH wild-type(A), and *IDH1* VUS / *IDH2* VUS *vs IDH* mutant(B). Panels (C–F), mass spec quantification of IDH-related metabolites: α-KG (C), 2-HG (D), L-2-HG (E), and D-2-HG (F) in *IDH* mutant, *IDH* VUS, *IDH* wild-type, and normal control plasma.

Conclusion: The *IDH* VUS included in our study, which were all predicted to have a pathogenic/damaging effect by DNA-based *in-silico* software, did not have the same 'canonical' ability to generate the oncometabolite 2-HG as *IDH* mutants and did not significantly impact survival outcomes. This is important when considering IDH-targeted therapies.

Nevertheless, our analysis of the VUS using specific IDH secondary structure and 3-D crystal structure-based models did corroborate the pathogenic/damaging effects offered by the original DNA-based *in-silico* software (predictive). These variants may still result in other lesser known effects on some other *IDH*-specific function. Along with providing an intermediate for the TCA cycle, IDH also contributes to the generation of NADPH which is important for lipid, amino acid, glucose biogenesis, and protection from oxidative and radiation-induced damage. Whether these changes are important or not to other aspects of cancer survival needs further assessment.

Declaration of Competing Interest

None.

Appendix A. Supplementary data

Supplementary material related to this article can be found, in the online version, at doi:https://doi.org/10.1016/j.leukres.2019.106264.

References

[1] W. Xu, et al., Oncometabolite 2-hydroxyglutarate is a competitive inhibitor of alpha-ketoglutarate-dependent dioxygenases, Cancer Cell 19 (1) (2011) 17–30.
[2] C.D. DiNardo, Ivosidenib in IDH1-mutated acute myeloid leukemia, N. Engl. J. Med. 379 (12) (2018) 1186.
[3] E.M. Stein, et al., Molecular remission and response patterns in patients with mutant-IDH2 acute myeloid leukemia treated with enasidenib, Blood 133 (7) (2019) 676–687.
[4] Z.J. Reitman, H. Yan, Isocitrate dehydrogenase 1 and 2 mutations in cancer: alterations at a crossroads of cellular metabolism, J. Natl. Cancer Inst. 102 (13) (2010) 932–941.
[5] A. Tefferi, et al., IDH1 and IDH2 mutation studies in 1473 patients with chronic-, fibrotic- or blast-phase essential thrombocythemia, polycythemia vera or myelofibrosis, Leukemia 24 (7) (2010) 1302–1309.
[6] E.R. Mardis, et al., Recurring mutations found by sequencing an acute myeloid leukemia genome, N. Engl. J. Med. 361 (11) (2009) 1058–1066.
[7] W.C. Chou, et al., The prognostic impact and stability of isocitrate dehydrogenase 2 mutation in adult patients with acute myeloid leukemia, Leukemia 25 (2) (2011) 246–253.
[8] N. Boissel, et al., Prognostic impact of isocitrate dehydrogenase enzyme isoforms 1 and 2 mutations in acute myeloid leukemia: a study by the Acute Leukemia French Association group, J. Clin. Oncol. 28 (23) (2010) 3717–3723.
[9] S. Abbas, et al., Acquired mutations in the genes encoding IDH1 and IDH2 both are recurrent aberrations in acute myeloid leukemia: prevalence and prognostic value, Blood 116 (12) (2010) 2122–2126.
[10] O. Kosmider, et al., Mutations of IDH1 and IDH2 genes in early and accelerated phases of myelodysplastic syndromes and MDS/myeloproliferative neoplasms, Leukemia 24 (5) (2010) 1094–1096.
[11] F. Thol, et al., IDH1 mutations in patients with myelodysplastic syndromes are associated with an unfavorable prognosis, Haematologica 95 (10) (2010) 1668–1674.
[12] A. Pardanani, et al., Recurrent IDH mutations in high-risk myelodysplastic syndrome or acute myeloid leukemia with isolated del(5q), Leukemia 24 (7) (2010) 1370–1372.
[13] G. Marcucci, et al., IDH1 and IDH2 gene mutations identify novel molecular subsets within de novo cytogenetically normal acute myeloid leukemia: a Cancer and Leukemia Group B study, J. Clin. Oncol. 28 (14) (2010) 2348–2355.
[14] P. Paschka, et al., IDH1 and IDH2 mutations are frequent genetic alterations in acute myeloid leukemia and confer adverse prognosis in cytogenetically normal acute myeloid leukemia with NPM1 mutation without FLT3 internal tandem duplication, J. Clin. Oncol. 28 (22) (2010) 3636–3643.
[15] M.M. Patnaik, et al., Prognostic interaction between ASXL1 and TET2 mutations in chronic myelomonocytic leukemia, Blood Cancer J. 6 (2016) e385.
[16] A.A. Zamyatnin, Protein volume in solution, Prog. Biophys. Mol. Biol. 24 (1972) 107–123.
[17] T. Dutta, et al., Impact of long-term poor and good glycemic control on metabolomics alterations in type 1 diabetic people, J. Clin. Endocrinol. Metab. 101 (3) (2016) 1023–1033.
[18] M.M. Koek, et al., Microbial metabolomics with gas chromatography/mass spectrometry, Anal. Chem. 78 (4) (2006) 1272–1281.
[19] W.M. Oldham, J. Loscalzo, Quantification of 2-hydroxyglutarate enantiomers by liquid chromatography-mass spectrometry, Bio Protoc. 6 (16) (2016).

[20] E.A. Struys, et al., Measurement of urinary D- and L-2-hydroxyglutarate enantiomers by stable-isotope-dilution liquid chromatography-tandem mass spectrometry after derivatization with diacetyl-L-tartaric anhydride, Clin. Chem. 50 (8) (2004) 1391–1395.

Alexander Tischer, Guadalupe Antelo, Giacomo Coltro, Christy M. Finke, Wilson Gonsalves, Animesh Pardanani
Division of Hematology, Department of Medicine, Mayo Clinic, Rochester, MN, USA

Rhett Ketterling
Department of Laboratory Medicine and Pathology, Mayo Clinic, Rochester, MN, USA

Abhishek Mangaonkar, Naseema Gangat, Ayalew Tefferi, Mrinal M. Patnaik, Terra L. Lasho*
Division of Hematology, Department of Medicine, Mayo Clinic, Rochester, MN, USA
E-mail address: lasho.terra@mayo.edu (T.L. Lasho).

* Corresponding author.